

# Molecular Structures of the Two Most Stable Conformers of Free Glycine

VERONIKA KASALOVÁ,<sup>1</sup> WESLEY D. ALLEN,<sup>1</sup> HENRY F. SCHAEFER III,<sup>1</sup> ESZTER CZINKI,<sup>2</sup> ATTILA G. CSÁSZÁR<sup>2</sup>

<sup>1</sup>Center for Computational Chemistry, University of Georgia, Athens, Georgia 30602-0525

<sup>2</sup>Laboratory of Molecular Spectroscopy, Institute of Chemistry, Eötvös University,  
H-1518 Budapest 112, Hungary

Received 9 June 2006; Revised 5 July 2006; Accepted 5 July 2006

DOI 10.1002/jcc.20680

Published online 6 March 2007 in Wiley InterScience (www.interscience.wiley.com).

**Abstract:** The equilibrium molecular structures of the two lowest-energy conformers of glycine, Gly-**I<sub>p</sub>** and Gly-**II<sub>n</sub>**, have been characterized by high-level ab initio electronic structure computations, including all-electron cc-pVTZ CCSD(T) geometry optimizations and 6-31G\* MP2 quartic force fields, the latter to account for anharmonic zero-point vibrational effects to isotopologic rotational constants. Based on experimentally measured vibrationally averaged effective rotational constant sets of several isotopologues and our ab initio data for structural constraints and zero-point vibrational shifts, least-squares structural refinements were performed to determine improved Born-Oppenheimer equilibrium ( $r_e$ ) structures of Gly-**I<sub>p</sub>** and Gly-**II<sub>n</sub>**. Without the ab initio constraints even the extensive set of empirical rotational constants available for 5 and 10 isotopologues of Gly-**I<sub>p</sub>** and Gly-**II<sub>n</sub>**, respectively, cannot satisfactorily fix their molecular structure. Excellent agreement between theory and experiment is found for the rotational constants of both conformers, the rms residual of the final fits being 7.8 and 51.6 kHz for Gly-**I<sub>p</sub>** and Gly-**II<sub>n</sub>**, respectively. High-level ab initio computations with focal point extrapolations determine the barrier to planarity separating Gly-**I<sub>p</sub>** and Gly-**II<sub>n</sub>** to be  $20.5 \pm 5.0$  cm<sup>-1</sup>. The equilibrium torsion angle  $\tau(\text{NCCO})$  of Gly-**II<sub>n</sub>**, characterizing the deviation of its heavy-atom framework from planarity, is  $(11 \pm 2)^\circ$ . Nevertheless, in the ground vibrational state the effective structure of Gly-**II<sub>n</sub>** has a plane of symmetry.

© 2007 Wiley Periodicals, Inc. J Comput Chem 28: 1373–1383, 2007

**Key words:** ab initio computations; equilibrium molecular structure; glycine; anharmonic force field; spectroscopic constants

## Introduction

Glycine (Gly) is the simplest naturally occurring amino acid, and thus one of the most fundamental molecules of biological interest. Gly is considered by many a prototypical amino acid in structural studies of peptides and proteins. Detection of glycine in interstellar space,<sup>1</sup> which most likely will involve its lowest-energy conformer Gly-**I<sub>p</sub>** (Fig. 1), is relevant to theories about the origin of molecules vital to life on Earth. Therefore, the molecular structures of the conformers of Gly, a neutral species in the gas phase, have been the focus of extensive experimental<sup>2–6</sup> and computational<sup>7–14</sup> studies. For a more complete list of work before 1992, see ref. 7.

There is consensus over the qualitative structural features of the two most stable conformers of glycine, **I** and **II** (Fig. 1). The notation employed in Figure 1 and throughout this paper follows that introduced in ref. 7, whereby **p** stands for a conformer (or conformation) having  $C_s$  point-group symmetry, **n** stands for a conformer having  $C_1$  point-group symmetry, and in

general Roman numerals, from **I** through **VIII**, indicate the relative stabilities of the conformers. Consequently, the two most stable conformers of Gly are denoted **I<sub>p</sub>** and **II<sub>n</sub>**,<sup>7</sup> having substantially different atomic arrangements.

Early on, around 1978, there was some confusion about the relative energies of the most stable conformers of Gly.<sup>2,6,14</sup> Theory, even at the low levels applicable in those days,<sup>14</sup> proved to be vital in the correct interpretation of the experimental microwave (MW) results and in proving that Gly-**I<sub>p</sub>** is the

**Correspondence to:** W. D. Allen; e-mail: wdallen@ccqc.uga.edu or A. G. Császár; e-mail: csaszar@chem.elte.hu

Contract/grant sponsor: U. S. National Science Foundation; contract/grant number: NSF-CHE04-51445

Contract/grant sponsor: Hungarian Scientific Research Fund; contract/grant number: OTKA T047185

Contract/grant sponsor: NSF-MTA-OTKA; contract/grant number: INT-0312355

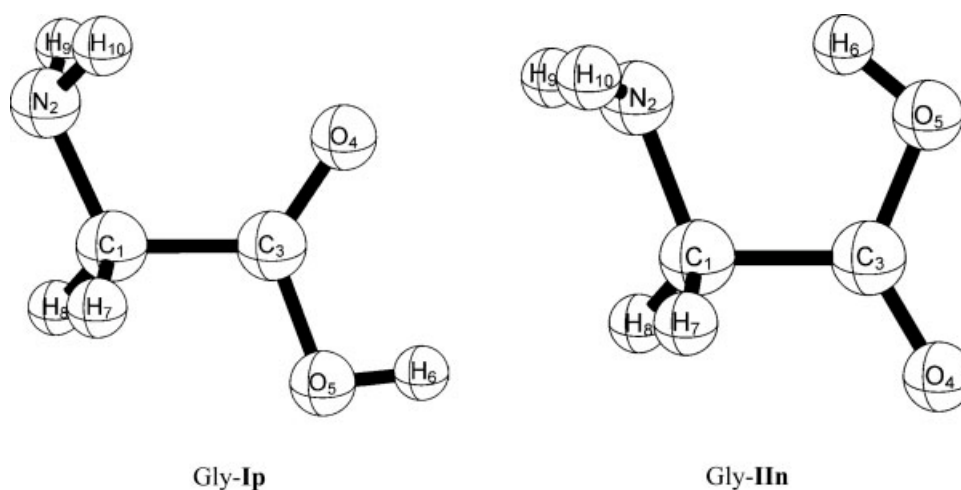


**Figure 1.** Structure of the two lowest-energy conformers of neutral glycine. The principal distortion of the Gly-IIa structure from planarity is an NCCO dihedral angle of 12.8° [cc-pVTZ CCSD(T) level].

global minimum on the potential energy surface (PES) of neutral Gly. For Gly-II, it remained unclear whether its equilibrium structure was planar or not. The determination of an extensive set of rotational constants of several isotopologues of Gly-II<sup>5</sup> was aided by the substantial dipole moments of this conformer. The empirical rotational constants of Gly-II indicated that the effective structure in the ground vibrational state is planar, because the amino hydrogens were indistinguishable in the partially deuterated [OH, NDH] and [OD, NDH] MW spectra. Electronic structure theory at most levels suggested<sup>7</sup> that the true equilibrium structure is nonplanar, though the energy difference between Gly-IIp and Gly-IIa was predicted to be only on the order of 20 cm<sup>-1</sup>. Despite the extensive experimental and theoretical data, the question of the (non)planarity of Gly-II was not definitely settled.

None of the studies performed up to now were able to obtain satisfactory Born-Oppenheimer equilibrium structures,  $r_e^{\text{BO}}$ , of Gly-Ip and Gly-IIa, quantities allowing direct comparison among disparate molecules. Furthermore, neither the gas electron diffraction (GED),<sup>4</sup> as detailed before,<sup>5,8</sup> nor the MW<sup>5</sup> and millimeterwave (MMW)<sup>6</sup> experimental studies yielded an accurate vibrationally averaged molecular structure of Gly-Ip. Application of the computational strategy of equilibrium structure determination of this study, outlined below, offers no difficulties for Gly-Ip, and the resulting  $r_e^{\text{BO}}$  structure should be highly reliable. For Gly-IIa both substitution ( $r_s$ ) and least-squares structures have been determined based on effective ground-state rotational constants of 12 isotopologues.<sup>5</sup> The  $r_s$  structure seemed to be suspect<sup>5</sup> due to “the small  $b$ -axis coordinates associated with both the nitrogen and carbonyl carbon atoms.” The least-squares structural fit assumed<sup>5</sup> that *in the ground vibrational state* Gly-IIa has  $C_s$  point-group symmetry. Nevertheless, no attempt was made in ref. 5 to derive the equilibrium structure of Gly-IIa, for which all dependable ab initio computations, including those of the present study, indicate a nonplanar atomic arrangement. Following our recent successful determination of the  $r_e^{\text{BO}}$  structure for the considerably larger and even less rigid

amino acid, L-proline,<sup>15</sup> here we report results of a similar study on the two lowest-energy conformers of neutral Gly.

### Computational Details

The computational strategy employed in this work, and recommended for similar studies to obtain highly reliable equilibrium structures, can be summarized as follows.

First, accurate values of  $r_e^{\text{BO}}$  are determined at advanced levels of electronic structure theory, in the present case at the all-electron (AE) cc-pVTZ CCSD(T) level (see below). Systematic investigations of the accuracy of computed molecular structures of 19 small closed-shell molecules containing first-row atoms were carried out by Helgaker and coworkers.<sup>16–18</sup> The mean absolute deviation (MAD) relative to experiment for the computed  $r_e$  bond distances was 0.0023 Å at the AE cc-pVTZ CCSD(T) level of theory. For AE cc-pVQZ CCSD(T), the mean absolute bond-length deviation was 0.0022 Å, only 0.0001 Å smaller than for cc-pVTZ CCSD(T). For bond angles, the MADs were 0.48 and 0.21° at the AE cc-pCVTZ CCSD(T) and cc-pCVQZ CCSD(T) levels of theory, respectively. These benchmarks show that for molecules containing first row atoms, cc-pVTZ CCSD(T) yields bond lengths and bond angles with accuracies in the range of 0.002 Å and 0.5°, respectively. Second, vibrational corrections between equilibrium and ground-state rotational constants are determined, in the present case at the all-electron 6-31G\* MP2 level, through computation of a full cubic force field and the use of second-order vibrational perturbation theory (VPT2).<sup>19–23</sup> A weakness of this standard approach is that no special consideration is given to large-amplitude motion(s). Third, the experimental ground-state rotational constants of all the isotopologues<sup>3,5</sup> are corrected to yield empirically-based equilibrium rotational constants. Fourth, guided weighted least-squares refinements are performed with various ab initio structural constraints to determine the  $r_e^{\text{BO}}$  parameters in best agreement with the available zero-point corrected experi-

**Table 1.** Valence Focal-Point Analysis of the Barrier to Planarity of Gly-**IIn** (cm<sup>-1</sup>).<sup>a,b,c</sup>

Basis	$E(\text{RHF})$	$\delta[\text{MP2}]$	$\delta[\text{CCSD}]$	$\delta[\text{CCSD(T)}]$	$\Delta E_c[\text{CCSD(T)}]$
aug-cc-pVDZ	64.12	-55.06	16.29	-9.84	15.51
aug-cc-pVTZ	61.22	-41.31	14.19	-8.62	25.47
aug-cc-pVQZ	61.99	-42.42	14.37	[-8.62]	[25.32]
aug-cc-pV5Z	61.84	-44.04	14.78	[-8.62]	[23.97]
CBS <sup>c</sup>	61.68	-45.74	15.22	[-8.62]	[22.54]

<sup>a</sup>The fixed reference structures employed for all the focal-point computations have been optimized at the all-electron cc-pVTZ CCSD(T) level.

<sup>b</sup>The symbol  $\delta$  denotes the increment in the relative energy ( $\Delta E_c$ ) with respect to the preceding level of theory, as given by the higher-order correlation series [HF  $\rightarrow$  MP2  $\rightarrow$  CCSD  $\rightarrow$  CCSD(T)]. The CCSD(T) correlation increments listed in brackets are taken for the purpose of extrapolation from corresponding entries for smaller basis sets, thus yielding the net  $\Delta E_c$  values also appearing in brackets.

<sup>c</sup>CBS, complete basis set limit. Based on  $X = (3, 4, 5)$  aug-cc-pVXZ RHF and  $X = (4, 5)$  aug-cc-pVXZ MP2 and CCSD energy points. See text for extrapolation formulas.

mental rotational constants. In particular, for Gly-**IIn** we decided to check carefully whether the experimental rotational constants can support an  $r_e^{\text{BO}}$  of  $C_1$  point-group symmetry.

### Electronic Structure Computations

Several correlated levels of electronic structure theory have been used previously in order to determine equilibrium structures of certain conformers of Gly. In ref. 7, geometry optimizations for all conformers of Gly were performed at the 6-311++G\*\* MP2 level, known to yield reasonably accurate equilibrium Born-Oppenheimer structures and rotational constants. In ref. 10, the highest-level optimizations were performed at the DZP CCSD level. The Born-Oppenheimer equilibrium structures of Gly-**I<sub>p</sub>**, Gly-**I<sub>p</sub>**, and Gly-**IIn** have been reoptimized in this study using the cc-pVTZ<sup>24</sup> basis set at the all-electron CCSD(T) level,<sup>25-27</sup> where CCSD(T) stands for coupled-cluster theory with all single and double excitations and a perturbative estimate of connected triple excitations. The geometry optimizations were performed with the program packages MOLPRO<sup>28</sup> and ACESII.<sup>29</sup>

The barrier to planarity of Gly-**IIn** was reported to be about 20 cm<sup>-1</sup> in previous work.<sup>7</sup> With such a minuscule barrier, we deemed it important to compute a definitive value for the **IIn**  $\rightarrow$  **I<sub>p</sub>** barrier to prove conclusively that this conformation is nonplanar. A valence focal-point analysis<sup>30-34</sup> of this quantity was thus executed, as detailed in Table 1. For the extrapolation of the Hartree-Fock energies, a three-parameter exponential formula,<sup>35,36</sup>

$$E_X^{\text{HF}} = E_\infty^{\text{HF}} + ae^{-bX} \quad (1)$$

was used, while for the extrapolation of the MP2 and CCSD electron correlation energies ( $\epsilon$ ), a two-parameter polynomial formula<sup>37</sup>

$$\epsilon_X^{\text{CC}} = \epsilon_\infty^{\text{CC}} + bX^{-3} \quad (2)$$

was employed. Energies computed with the aug-cc-pVXZ ( $X = T, Q, 5$ ) basis sets<sup>24,38-41</sup> were used in the extrapolations. Core

correlation shifts were determined at the cc-pCVTZ<sup>24,41</sup> CCSD(T) level of theory.

To account for zero-point vibrational effects in the experimental rotational constants, anharmonic force field expansions of the vibrational potential energy surface were computed for Gly-**I<sub>p</sub>** and Gly-**IIn** in normal coordinates<sup>42,43</sup> at the all-electron MP2 level with the 6-31G\* basis set,<sup>44</sup> employing the code ACESII.<sup>29</sup> In our previous work on proline,<sup>15</sup> we found the 6-31G\* MP2 method to be both a sufficiently accurate and economical approach to computing zero-point vibrational effects on the structures of larger molecules. To ensure accuracy of the anharmonic force fields of glycine, geometries were tightly optimized to better than 10<sup>-6</sup> Å and 10<sup>-5</sup> degrees, and analytic second derivative techniques were invoked.<sup>45</sup> The force fields were computed at the respective equilibrium structures in order to avoid the nonzero force dilemma.<sup>46</sup> In determining the total vibrational contributions to ground-state rotational constants, Coriolis resonances need not be considered because all resonance denominators cancel in the summation over normal modes. For the Gly-**I<sub>p</sub>** transition state, in-house programs were used to compute anharmonic force constants. The program INTDIF2004<sup>47</sup> was employed to determine the required displacements as well as compute the force constants in internal coordinates. The transformation of the force constants from internal to normal coordinates and the computation of spectroscopic constants were performed using the programs INTDER2000<sup>48,49</sup> and ANHARM,<sup>50</sup> respectively.

\*INTDIF2004 is an abstract program developed by Allen, W. D. for use within *Mathematica* (Wolfram Research Inc., Champaign, Illinois) to perform high-order numerical differentiations of electronic structure data.

†INTDER2000 is a general program developed by Allen, W. D. and coworkers which performs various vibrational analyses and higher-order nonlinear transformations among force field representations.

‡ANHARM is a FORTRAN program written for VPT2 analyses by Yamaguchi, Y. and Schaefer, H. F. (Center for Computational Chemistry, University of Georgia, Athens, GA 30602, USA). See program description in Ref. 50.

**Table 2.** Equilibrium ( $A_e$ ,  $B_e$ ,  $C_e$ ) and Effective ( $A_0$ ,  $B_0$ ,  $C_0$ ) Rotational Constants (in MHz) for the Parent Isotopologues of Gly-**I**p, Gly-**II**p, and Gly-**II**n.

	$A_e[A_0]$	$B_e[B_0]$	$C_e[C_0]$
<b>Gly-<b>I</b>p</b>			
6-311++G** MP2 <sup>a</sup>	10279.0	3877.0	2908.1
6-31G* MP2 (AE)	10228.1[10149.4]	3893.5[3862.2]	2912.8[2890.5]
cc-pVTZ CCSD(T)(AE) <sup>b</sup>	10407.5[10328.8]	3914.0[3882.7]	2937.5[2915.2]
Expt. <sup>c</sup>	[10341.521(89)]	[3876.1785(12)]	[2912.3509(10)]
<b>Gly-<b>II</b>p</b>			
6-311++G** MP2 <sup>a</sup>	10175.1	4076.3	3010.9
6-31G* MP2 (AE)	10119.5[10023.7]	4071.9[4049.4]	3003.7[2982.6]
cc-pVTZ CCSD(T) (AE) <sup>b</sup>	10255.0[10159.2]	4097.0[4074.5]	3028.0[3006.9]
<b>Gly-<b>II</b>n</b>			
6-311++G** MP2 <sup>a</sup>	10127.5	4085.3	3024.8
6-31G* MP2 (AE)	10022.9[9957.2]	4093.3[4059.4]	3031.3[2998.9]
cc-pVTZ CCSD(T) (AE) <sup>b</sup>	10182.8[10117.1]	4112.6[4078.7]	3045.3[3012.9]
Expt. <sup>c</sup>	[10129.86(34)]	[4071.497(11)]	[3007.485(11)]

<sup>a</sup>Ref. 7.<sup>b</sup>The cc-pVTZ CCSD(T)  $A_0$ ,  $B_0$ , and  $C_0$  values were determined using cc-pVTZ CCSD(T) equilibrium  $A_e$ ,  $B_e$ , and  $C_e$  rotational constants and 6-31G\* MP2 vibrational corrections (Table 9 below).<sup>c</sup>Effective ground-state values, Ref. 3.

### Structural Refinements

With the aid of our fully optimized all-electron cc-pVTZ CCSD(T) structures, we undertook a weighted least-squares refinement (LSR) to determine improved equilibrium structural parameters for Gly-**I**p and Gly-**II**n. We used the reciprocal statistical uncertainties of the experimental rotational constants as specific weights for each rotational constant. We exclusively employed a *Mathematica* program MolStruct<sup>15</sup> during this study for the LSRs.

Upon constraining diverse sets of internal coordinates to their cc-pVTZ CCSD(T) equilibrium values and then performing LSR on the rest, we were always able to achieve facile convergence in the fit for Gly-**I**p, in the final run with a root-mean-square (rms) deviation of only 7.8 kHz. The situation was more difficult for the LSR of Gly-**II**n, but after careful selection of structural constraints we were able to achieve convergence with an rms error of only 51.6 kHz even for this conformer. The assumption of a planar Gly-**II**p structure led to a large deterioration of the fit. More detailed description of the weighted least-squares refinement procedures and results for Gly-**I**p, Gly-**II**p, and Gly-**II**n are given in the following section.

### Results and Discussion

Owing to sizable vibrational averaging effects, the directly computed ab initio equilibrium Born-Oppenheimer rotational constants ( $A_e$ ,  $B_e$ ,  $C_e$ ) may deviate substantially from the experimen-

tally measured ground-state ones ( $A_0$ ,  $B_0$ ,  $C_0$ ). To wit, the all-electron 6-31G\* MP2 and cc-pVTZ CCSD(T) equilibrium rotational constants of Gly-**I**p and Gly-**II**n (Table 2) display differences as large as 113 MHz from the experimental rotational constants. The corrections for vibrational averaging computed from the all-electron 6-31G\* MP2 anharmonic force field, amounting to 0.7–1.1% of the equilibrium rotational constants for the parent isotopologue, reduce the deviations from experiment by an order of magnitude, in accord with the good accuracy usually observed<sup>15,19,20,51–53</sup> for theoretical vibration–rotation interaction ( $\alpha_i$ ) constants. As mentioned earlier, standard VPT2 computations of  $\alpha_i$  constants do not give special consideration to large-amplitude motions in double-well potentials, as encountered here for Gly-**II**. For most of the modes in Gly-**II**, the use of  $\alpha_i$  constants to account for zero-point vibrational averaging should be satisfactory. The overall success of the entire set of  $\alpha_i$  constants in bringing the experimental and theoretical rotational constants into accord is a test of the efficacy of the VPT2 approach under problematic conditions.

The computed differences between the vibrationally-averaged rotational constants of the parent isotopologue and those of the substituted ones of Gly-**I**p, as reported in Table 3, reproduce remarkably well the experimentally measured differences. The situation is not so clear for Gly-**II**n (Table 4). McGlone et al.<sup>5</sup> reported 12 sets of effective rotational constants for Gly-**II**n isotopologues. For 10 of these the agreement is about as good for Gly-**II** as for Gly-**I**p. However, for the substitutions [OH,NDH] and [OD,NDH] relatively large discrepancies are observed between the computed and measured rotational constant shifts. These disparities are related to the inability to measure the rotational constants corresponding to the individual isotopomers NDH/NHD. The effective rotational constants determined by

\*MolStruct is an abstract program developed by Allen, W. D. for use within *Mathematica* (Wolfram Research Inc., Champaign, Illinois) to perform diverse fits of molecular structures to sets of isotopologic rotational constants.

**Table 3.** Theoretical and Experimental (in brackets) Isotopic Shifts of the Vibrationally Averaged Rotational and the *A*-Reduced Quartic Centrifugal Distortion Constants of Isotopologues of Gly-**Ip**.<sup>a</sup>

	Parent	<sup>13</sup> C(3)	<sup>13</sup> C(1)	C(1)-d <sub>2</sub>	<sup>15</sup> N	MAD <sup>b</sup>
<i>A</i> <sub>0</sub> (MHz)	10149.4 [10341.5]	-0.6 [-0.6]	-112.8 [-114.4]	-999.2 [-1023.1]	-0.1 [-0.1]	6.4
<i>B</i> <sub>0</sub> (MHz)	3862.2 [3876.2]	-7.1 [-7.0]	-17.0 [-17.1]	-77.5 [-76.9]	-113.5 [-113.7]	0.3
<i>C</i> <sub>0</sub> (MHz)	2890.5 [2912.4]	-4.0 [-4.0]	-18.8 [-18.6]	-80.2 [-80.0]	-64.0 [-64.7]	0.3
<i>D</i> <sub>J</sub> (kHz)	0.7629 [0.7434]	-0.0020 [-0.007]	<b>-0.0091 [-0.10]</b>	-0.0097 [-0.007]	<b>-0.0355 [+0.45]</b>	
<i>D</i> <sub>JK</sub> (kHz)	3.4513 [3.986]	<b>+0.0044 [+0.07]</b>	<b>-0.2429 [-0.0]</b>	-1.4293 [-1.5]	<b>-0.0599 [-0.9]</b>	
<i>D</i> <sub>K</sub> (kHz)	<b>3.5700 [0]<sup>c</sup></b>	+0.0195 [d]	-0.1427 [d]	<b>-1.1960 [0]<sup>c</sup></b>	<b>0.0946 [0]<sup>c</sup></b>	
<i>d</i> <sub>1</sub> (kHz)	-0.1853 [-0.1901]	+0.0007 [+0.002]	<b>-0.0014 [-0.03]</b>	+0.0017 [+0.006]	<b>+0.0121 [-0.22]</b>	
<i>d</i> <sub>2</sub> (kHz)	-0.0173 [-0.0158]	+0.0000 [-0.004]	-0.0003 [0] <sup>c</sup>	+0.0255 [+0.022]	0.0010 [0] <sup>c</sup>	

<sup>a</sup>Values obtained at the 6-31G\* MP2 (AE) level of theory. Shifts in the rotational constants of the isotopologues are given relative to the absolute values listed for the parent. Measured effective quantities from Ref. 3 are given, for the ease of visualization, in brackets; see Table 1 therein for uncertainties. All theoretical rotational constants include 6-31G\* MP2 (AE) zero-point vibrational corrections (see Table 2). See Figure 1 for numbering of the atoms. Points of significant disparity between theory and experiment are printed in boldface.

<sup>b</sup>Mean absolute difference between theoretical and experimental isotopic shifts for the rotational constants.

<sup>c</sup>Absolute quantities were constrained to zero.

<sup>d</sup>Absolute theory [expt.] *D*<sub>K</sub> quantities are 3.59 [4.8] for <sup>13</sup>C(3) and 3.43[11.0] for <sup>13</sup>C(1).

McGlone et al.<sup>5</sup> correspond to neither isotopomer of this *C*<sub>1</sub>-symmetry conformer but to a vibrational average. When these rotational constants were included in the set of experimental observables, unacceptably large fitting errors resulted. The anomalous rotational constants of [OH,NDH] and [OD,NDH] were therefore not employed in the final structural fits here.

For both Gly-**Ip** and Gly-**IIn** changes in the isotopically substituted quartic centrifugal distortion constants presented in Tables 3 and 4, respectively, mostly support the data of Godfrey and Brown.<sup>3</sup> The discrepancies highlighted in Tables 3 and 4 are probably due to both the limited number of lines observed for some of the isotopologues and the effective nature of the experimental constants.

#### Least-Squares Refinement for Gly-**Ip**

Although the isotopologic rotational constant data for Gly-**Ip** are extensive, they are clearly insufficient to give a well-defined structure without the imposition of constraints. There are 15 structural degrees of freedom for planar Gly-**Ip**, and 15 empirical rotational constants in the experimental data set.

Having all-electron cc-pVTZ CCSD(T) optimum structural parameters, we are in a position to impose realistic and reliable constraints on the structural refinement of Gly-**Ip**, as specified in Table 5. With all parameters fixed, the variables that are best determined from the input rotational constants are identified on the basis of the least-squares Hessian. Candidates for constraint release are relaxed one by one, and new determinants of the least-squares Hessian are evaluated. Using this automatic procedure to predict the parameters to be optimized, we found that it is best to start the fitting procedure with the four heavy-atom distances relaxed while keeping the rest of the internal coordinates fixed at their cc-pVTZ CCSD(T) optimum values. Somewhat to our surprise, the corrected empirical rotational constants can be fit quite well this way; the weighted rms error is 0.216 MHz and no residual is over 2 MHz. The corresponding results are listed under *r*<sub>e</sub>(Fit 1) in Table 6.

The structure of Gly-**Ip** can be improved by performing additional fits with further relaxation of constraints. More variables are selected and released using the procedure outlined earlier. In the end, only four structural constraints are required, as listed in Table 5. Of these constraints, *r*(O—H) and  $\theta$ (C—O—H) are not well defined by the data, which is not surprising since no deuterium substitution information is available for the hydroxyl group. Similarly, no rotational constants are available for the NHD and ND<sub>2</sub> substitutions; therefore  $\theta$ (NH<sub>2</sub> scissor) and  $\theta$ (NH<sub>2</sub> wag) are not defined well by the data and need to be constrained as well. The *r*(N—H) bond length was released because it led to a small decrease in the rms error.

Results from the final structural refinement for Gly-**Ip** are presented in Table 6 as *r*<sub>e</sub>(Fit 2). Deviations between the fitted empirical and all-electron cc-pVTZ CCSD(T) *r*<sub>e</sub><sup>BO</sup> structures of Gly-**Ip** are comfortably small. For bond lengths, the largest difference is 0.006 Å for the N—H bond, which is due to the limited data available to fit this variable, as noted earlier. The value of  $\theta$ (C—C—O) in Fit 2 differs from the cc-pVTZ CCSD(T) value by 0.5°, while deviations for the other angles are considerably smaller. This verifies the generally accepted predictive power of structure optimizations at high levels of electronic structure theory.

There are significant discrepancies between the *r*<sub>α</sub><sup>0</sup> parameters derived from gas-phase electron diffraction (GED) data<sup>4</sup> and our fitted *r*<sub>e</sub> parameters (Table 6). Considerable problems with this GED investigation have been addressed previously by Császár<sup>7,8</sup> and are not elaborated on further here.

#### Barrier to Planarity of Gly-**IIn**

Before the structural refinement of the second lowest-lying conformer of glycine, Gly-**IIn**, we determined the energy difference between Gly-**Ip** and Gly-**IIn** using the technique of focal-point analysis (FPA).<sup>30–34</sup> The FPA valence-only increments are listed in Table 1. Because the basis set extrapolations are converged well (within 2 cm<sup>-1</sup>), the error bars for the barrier to planarity

**Table 4.** Theoretical and Experimental (in brackets) Isotopic Shifts of the Vibrationally Averaged Rotational and Quartic Centrifugal Distortion Constants of Gly-**1In**.<sup>a</sup>

Parent	<sup>15</sup> N	<sup>13</sup> C(2)	<sup>13</sup> C(1)	C= <sup>18</sup> O	H- <sup>18</sup> O	OD, NH <sub>2</sub>	CD <sub>2</sub>	OH, NHD <sup>b</sup>	OH, ND <sub>2</sub>	OD, NHD <sup>c</sup>	OD, ND <sub>2</sub>
A <sub>0</sub>	9957.2 [10129.9]	-133.1 [-133.7]	0.5 [0.8]	-126.0 [-129.2]	-599.7 [-609.8]	-381.0 [-397.7]	-1031.5 [-1049.3]	-202.4 [-131.1]	-269.4 [-265.9]	-569.2 [-520.1]	-633.5 [-645.1]
B <sub>0</sub>	4059.4 [4071.5]	-16.6 [-16.4]	-11.6 [-11.7]	-175.2 [-173.6]	-13.4 [-14.3]	-9.9 [-9.0]	-83.8 [-82.5]	-181.2 [-203.2]	-380.3 [-385.8]	-189.2 [-210.2]	-386.4 [-391.4]
C <sub>0</sub>	2998.9 [3007.5]	-20.6 [-20.7]	-6.3 [-6.3]	-107.2 [-106.6]	-63.8 [-63.8]	-40.3 [-40.7]	-89.6 [-89.9]	-82.1 [-101.1]	-191.5 [-194.8]	-119.6 [-138.7]	-226.0 [-229.5]
D <sub>J</sub>	0.7200 [0.665]	-0.0094 [+0.070]	-0.0025 [-0.0060]	-0.0742 [-0.069]	-0.0086 [+0.086]	-0.0236 [-0.099]	-0.0374 [+0.063]	+0.0625 [+0.1370]	-0.0826 [-0.0040]	+0.0373 [+0.0960]	-0.1007 [+0.0140]
D <sub>JK</sub>	2.5009 [4.81]	-0.1115 [-0.48]	-0.0149 [-0.03]	-0.3108 [-0.38]	+0.1273 [-0.38]	+0.1050 [+0.38]	-0.7635 [-0.81]	-0.7717 [+0.04]	-0.0256 [+3.77]	-0.6509 [+0.33]	+0.0584 [0] <sup>d</sup>
D <sub>K</sub>	6.6020 [-28]	+0.1737 [0] <sup>d</sup>	+0.0169 [0] <sup>d</sup>	+0.8306 [0] <sup>d</sup>	-1.4526 [0] <sup>d</sup>	-0.1613 [0] <sup>d</sup>	-2.6481 [+23]	+1.3808 [0] <sup>d</sup>	-0.5470 [0] <sup>d</sup>	+1.1363 [0] <sup>d</sup>	-0.6746 [+36]
d <sub>1</sub>	-0.1524 [-0.167]	+0.0086 [-0.034]	+0.0008 [+0.037]	+0.0194 [+0.003]	-0.0081 [-0.052]	+0.0022 [+0.062]	+0.0067 [+0.012]	+0.0164 [-0.020]	+0.0368 [+0.014]	+0.0170 [+0.023]	+0.0374 [-0.004]
d <sub>2</sub>	-0.0421 [0.039]	+0.0030 [0] <sup>d</sup>	+0.0004 [0] <sup>d</sup>	+0.0068 [0] <sup>d</sup>	-0.0062 [0] <sup>d</sup>	-0.0023 [0] <sup>d</sup>	+0.0123 [-0.0045]	+0.0126 [0] <sup>d</sup>	+0.0180 [0] <sup>d</sup>	+0.0106 [0] <sup>d</sup>	+0.0158 [0] <sup>d</sup>

<sup>a</sup>Values obtained at the 6-31G\* MP2 (AE) level of theory. See Figure 1 for numbering of the atoms. The units assumed for the vibrationally averaged rotational constants and the A-reduced quartic centrifugal distortion constants are MHz and kHz, respectively. Shifts are given for the isotopically substituted species relative to the absolute values listed for the parent molecule. For the centrifugal distortion constants, equilibrium 6-31G\* MP2(AE) values are listed first. Measured effective quantities from Refs. [3,5] appear in brackets. See original paper for uncertainties. All theoretical rotational constants include 6-31G\* MP2(AE) zero-point vibrational corrections. Points of significant disparity are printed in boldface for easier visualization. The mean absolute difference between theoretical and experimental isotopic shifts for the rotational constants is (7.2, 1.8, 1.0) MHz for (A<sub>0</sub>, B<sub>0</sub>, C<sub>0</sub>); the statistics exclude the outlying data for the (OH,NDH) and (OD,NDH) isotopologues.

<sup>b</sup>The theoretical differences corresponding to the H<sub>9</sub>D<sub>10</sub> substituted isotopologue are listed in the table, while the same values are for the D<sub>9</sub>H<sub>10</sub> substituted isotopologue are (-57.3, -221.5, -118.5) MHz for (A<sub>0</sub>, B<sub>0</sub>, C<sub>0</sub>).

<sup>c</sup>The theoretical differences corresponding to the D<sub>6</sub>H<sub>3</sub>D<sub>10</sub> substituted isotopologue are listed in the table, while the same values for the D<sub>6</sub>D<sub>9</sub>H<sub>10</sub> substituted isotopologue are (-436.6, -228.9, -155.4) MHz for (A<sub>0</sub>, B<sub>0</sub>, C<sub>0</sub>).

<sup>d</sup>Absolute quantities for these isotopologues were constrained to zero.

**Table 5.** Structural Constraints Employed in the Final Structural Fits for Gly-**I**p and Gly-**II**n.<sup>a</sup>

Gly- <b>I</b> p	Gly- <b>II</b> n
1. $r(\text{O}-\text{H}) = 0.9660$	1. $\Delta r(\text{C}-\text{H}) = -0.000189$
2. $\theta(\text{C}-\text{O}-\text{H}) = 106.04^\circ$	2. $\Delta r(\text{N}-\text{H}) = -0.00170$
3. $\theta(\text{NH}_2 \text{ scissor}) = 104.98^\circ$	3. $\Delta\theta(\text{CH}_2 \text{ rock})^b = 0.116^\circ$
4. $\gamma(\text{NH}_2 \text{ wag})^b = 57.67^\circ$	4. $\Delta\theta(\text{CH}_2 \text{ twist})^b = 0.0642^\circ$
	5. $\tau(\text{HNCC av})^b = 5.43^\circ$

<sup>a</sup>Units are Å for distances ( $r$ ) and degrees for bond ( $\theta$ ), torsional ( $\tau$ ), and out-of-plane ( $\gamma$ ) angles.

<sup>b</sup> $\gamma(\text{NH}_2 \text{ wag}) =$  bending angle of  $\text{C}_1-\text{N}_2$  out of  $\text{N}_2\text{H}_5\text{H}_{10}$  plane;  $\Delta\theta(\text{CH}_2 \text{ rock}) = \theta(8,1,2) + \theta(8,1,3) - \theta(7,1,2) - \theta(7,1,3)$ ;  $\Delta\theta(\text{CH}_2 \text{ twist}) = \theta(8,1,2) - \theta(8,1,3) - \theta(7,1,2) + \theta(7,1,3)$ ;  $\tau(\text{HNCC av}) = \tau(10,2,1,3) + \tau(9,2,1,3)$ . See Figure 1 for atom numbering.

are determined from the less converged extrapolation of the correlation effects. The correlation energy increments at the complete basis set (CBS) limit at the MP2, CCSD, and CCSD(T) levels change as  $-46 \text{ cm}^{-1}$ ,  $+15 \text{ cm}^{-1}$ , and  $-9 \text{ cm}^{-1}$ , respectively. Following this behavior, we estimate the uncertainty for the barrier to planarity resulting from neglect of higher-order excitations to be  $\pm 5 \text{ cm}^{-1}$ . The results of Table 1 show definitively that at equilibrium Gly-**II** is nonplanar. After including core-correlation shifts ( $-2.07 \text{ cm}^{-1}$ ), our best estimate for the classical barrier to planarity for the equilibrium structure of Gly-**II**n is  $20.5 \pm 5.0 \text{ cm}^{-1}$ .

Zero-point vibrational effects on the barrier to planarity of Gly-**II**n are complicated and cannot be accounted for by a simple one-dimensional model. The lowest vibrational frequencies of Gly-**II**n and Gly-**II**p are  $(104, 287) \text{ cm}^{-1}$  and  $(102i, 228) \text{ cm}^{-1}$ , respectively, at the 6-31G\* MP2 level of theory. In each structure, both modes involve strong mixtures of

$\text{N}-\text{C}-\text{C}-\text{O}$  backbone torsional motion with internal rotation of the  $\text{NH}_2$  group about the  $\text{N}-\text{C}$  bond. Only one other frequency lies below  $500 \text{ cm}^{-1}$ , corresponding to a bending deformation of the  $\text{N}-\text{C}-\text{C}-\text{O}$  backbone. This third vibration, at  $341$  and  $346 \text{ cm}^{-1}$  for Gly-**II**n and Gly-**II**p, respectively (6-31G\* MP2), is of  $a'$  symmetry in the planar structure and is thus uncoupled to the two lowest-frequency modes. If the harmonic ZPVE of the 22 highest-frequency vibrations is considered, the effect on the barrier to planarity is only  $-7 \text{ cm}^{-1}$ , owing to a cancellation of several more sizable contributions. If the second lowest frequency [ $\nu_{23}(a'')$ ] is included, the ZPVE shift is  $-37 \text{ cm}^{-1}$ , which would cancel out the  $20.5 \text{ cm}^{-1}$  classical barrier. However, adding  $\nu_{23}$  into the ZPVE computation is not well justified because its similarity in time scale and strong coupling to  $\nu_{24}$  vitiates a sudden/adiabatic separation of the two lowest frequency modes of Gly-**II**. An adequate description of Gly-**II** would require at least a two-dimensional dynamical model involving a nonplanar minimum, an effective barrier to planarity less than  $20 \text{ cm}^{-1}$ , and a ground vibrational state that surely surmounts this barrier.

#### Least-Squares Refinement for Gly-**II**n

As a starting point, we attempted to reproduce the structural parameters from a least-squares fit reported by McGlone et al.,<sup>5</sup> by performing an unconstrained LSR of a planar structure with no vibrational corrections to the rotational constants. All 12 isotopologues were used in the fit, which is designated as  $r_0(\text{Fit A})$  in Table 7. The parameters  $r_0(\text{C}-\text{N})$ ,  $r_0(\text{C}=\text{O})$ ,  $r_0(\text{C}-\text{O})$ ,  $r_0(\text{O}-\text{H})$ ,  $r_0(\text{C}-\text{H av})$ ,  $\theta_0(\text{C}-\text{O}-\text{H})$ , and  $\theta_0(\text{C}-\text{C}-\text{O})$  are identical to the number of digits reported in ref. 5. Among the other structural parameters, the largest differences are  $0.018 \text{ \AA}$  and  $1.2^\circ$  for the  $r_0(\text{C}-\text{C})$  bond length and the  $\theta_0(\text{CH}_2 \text{ scissor})$  angle, respectively. These deviations are still well within the

**Table 6.** Structural Parameters of Gly-**I**p.<sup>a</sup>

	Expt. <sup>b</sup> $r_s$	Expt. <sup>c</sup> $r_\alpha^0$	cc-pVTZ CCSD(T)	$r_e(\text{Fit 1})^d$	$r_e(\text{Fit 2})^e$ Final
$r(\text{C}-\text{N})$	1.468	1.466(6)	1.446	1.448(4)	<b>1.441(1)</b>
$r(\text{C}-\text{C})$	1.485	1.529(4)	1.511	1.514(2)	<b>1.511(1)</b>
$r(\text{C}=\text{O})$	–	1.204(1)	1.204	1.203(1)	<b>1.207(2)</b>
$r(\text{C}-\text{O})$	–	1.354(2)	1.349	1.347(4)	<b>1.353(1)</b>
$r(\text{C}-\text{H})$	1.082	1.081	1.088	–	<b>1.0907(2)</b>
$r(\text{N}-\text{H})$	–	1.001	1.012	–	<b>1.0065(2)</b>
$\theta(\text{C}-\text{C}-\text{O})$	–	111.5(2)	111.4	–	<b>111.9(1)</b>
$\theta(\text{O}-\text{C}-\text{O})$	–	123.5(5)	123.1	–	<b>123.2(1)</b>
$\theta(\text{C}-\text{C}-\text{N})$	115.1	113.0(3)	115.2	–	<b>115.4(1)</b>
$\theta(\text{CH}_2 \text{ scissor})$	106.2	–	105.9	–	<b>105.95(3)</b>
$\theta(\text{CH}_2 \text{ wag})$	6.1	–	5.1	–	<b>5.4(1)</b>
rms residual(kHz)				216	7.8

<sup>a</sup>Units are Å for distances ( $r$ ) and degrees for bond angles ( $\theta$ ). Standard errors of the weighted least-squares fit are given in parentheses. The weights in the fits to the experimental rotational constants are set to the reciprocal uncertainties.

<sup>b</sup>Derived from Kraitchman coordinates reported in Ref. 3.

<sup>c</sup>Ref. 4. See also Ref. 5.

<sup>d</sup>Fit 1 releases  $r(\text{C}-\text{N})$ ,  $r(\text{C}-\text{C})$ ,  $r(\text{C}=\text{O})$ , and  $r(\text{C}-\text{O})$  only.

<sup>e</sup>Fit 2 imposes the constraints listed in Table 5.

Table 7. Structural Parameters of Gly-**II**n.<sup>a</sup>

	Expt. <sup>b</sup> $r_s$	Expt. <sup>c</sup> $r_0$	cc-pVTZ CCSD(T)	$r_0$ (Fit A) <sup>d</sup>	$r_0$ (Fit B) <sup>e</sup>	$r_c$ (Fit 1) <sup>f</sup>	$r_c$ (Fit 2) <sup>f</sup>	$r_c$ (Fit 3) <sup>f</sup> Final
$r(\text{C}-\text{C})$	1.545	1.52(3)	1.524	1.538(16)	1.540(7)	1.522(6)	1.525(1)	<b>1.524(2)</b>
$r(\text{C}-\text{N})$	1.459	1.46(3)	1.463	1.461(30)	1.460(11)	1.466(6)	1.462(2)	<b>1.462(2)</b>
$r(\text{C}=\text{O})$	1.228	1.21(2)	1.201	1.210(16)	1.210(6)	1.197(5)	1.201(1)	<b>1.202(2)</b>
$r(\text{C}-\text{O})$	1.291	1.33(4)	1.337	1.329(22)	1.326(9)	1.340(7)	1.333(1)	<b>1.333(2)</b>
$r(\text{O}-\text{H})$	0.993	0.98(2)	0.977	0.976(17)	0.999(8)	0.996(7)	0.991(1)	<b>0.992(2)</b>
$r(\text{C}-\text{H av})$	1.098	1.10(2)	1.087	1.099(7)	1.100(3)	1.084(3)	1.084(1)	<b>1.084(1)</b>
$r(\text{N}-\text{H av})$	1.000	1.01(2)	1.009	1.004(20)	1.003(8)	1.013(2)	1.012(2)	<b>1.014(3)</b>
$\theta(\text{C}-\text{O}-\text{H})$	104.8	105(1)	104.4	104.8(9)	104.8(4)	104.9(3)	105.2(1)	<b>105.2(1)</b>
$\theta(\text{C}-\text{C}-\text{O})$	116.1	115(2)	113.8	115.0(11)	114.9(4)	114.0(4)	114.2(1)	<b>114.3(1)</b>
$\theta(\text{O}-\text{C}-\text{O})$	–	–	123.5	123.8(17)	124.0(7)	122.9(6)	123.4(1)	<b>123.3(2)</b>
$\theta(\text{C}-\text{C}-\text{N})$	110.6	112.2	111.2	111.4(12)	111.4(5)	111.3(3)	111.3(2)	<b>111.4(2)</b>
$\theta(\text{CH}_2 \text{ scissor})$	107.4	107(2)	107.3	108.2(10)	108.3(4)	106.4(4)	106.6(2)	<b>106.7(2)</b>
$\Delta\theta(\text{CH}_2 \text{ wag})^g$	–	–	10.4	10.9(33)	10.8(13)	8.7(10)	7.9(2)	<b>8.0(4)</b>
$\theta(\text{NH}_2 \text{ scissor})$	112.5	110(3)	107.2	111.2(33)	110.9(13)	105.9(5)	107.0(7)	<b>107.0(11)</b>
$\tau(\text{NCCO})$	–	–	12.8	–	–	12.3(15)	12.1(13)	<b>11.2(19)</b>
$\tau(\text{CCOH})$	–	–	–2.3	–	–	–2.9(37)	–3.4(15)	<b>–2.5(19)</b>
$\gamma(\text{NH}_2 \text{ wag})^g$	–	–	52.5	43.7(331)	43.7(127)	–	48.4(15)	<b>48.5(23)</b>
$\Delta\theta(\text{NH}_2 \text{ rock})^g$	–	–	0.4	–	–	–	7.2(10)	<b>8.0(17)</b>
$\gamma(\text{COOH wag})^{g,h}$	–	–	–1.3	–	–	–	–	<b>0.12(286)</b>
rms residual(kHz)				724	437	303	52.9	51.6

<sup>a</sup>Units are Å for distances ( $r$ ) and degrees for bond ( $\theta$ ), torsional ( $\tau$ ), and out-of-plane ( $\gamma$ ) angles. Standard errors of the weighted least-squares refinement are given in parentheses. The weights in the fits to the experimental rotational constants are set to the reciprocal uncertainties.

<sup>b</sup>Substitution structure from Ref. 5.

<sup>c</sup>Structure from an unconstrained least-squares fit from Ref. 5.

<sup>d</sup>Planar  $r_0$  structure with all 12 isotopologues included in the fit; no constraints other than those which define planarity were imposed.

<sup>e</sup>Planar  $r_0$  structure with [OH,NDH] and [OD,NDH] isotopologues excluded from the fit; no constraints other than those which define planarity were imposed.

<sup>f</sup>Nonplanar  $r_c$  structure with [OH,NDH] and [OD,NDH] isotopologues excluded from the fits; Fits 1 and 2 impose the constraints listed in Table 5 and, in addition, [ $\gamma(\text{NH}_2 \text{ wag})$ ,  $\Delta\theta(\text{NH}_2 \text{ rock})$ ,  $\gamma(\text{COOH wag})$ ] and [ $\gamma(\text{COOH wag})$ ], respectively. Fit 3 imposes only the constraints listed in Table 5.

<sup>g</sup> $\Delta\theta(\text{CH}_2 \text{ wag}) = \theta(8,1,2) - \theta(8,1,3) + \theta(7,1,2) - \theta(7,1,3)$ ;  $\gamma(\text{NH}_2 \text{ wag}) =$  bending angle of  $\text{C}_1-\text{N}_2$  out of  $\text{N}_2\text{H}_{10}\text{H}_9$  plane;  $\Delta\theta(\text{NH}_2 \text{ rock}) = \theta(1,2,10) - \theta(1,2,9)$ ;  $\gamma(\text{COOH wag}) =$  bending angle of  $\text{C}_1-\text{C}_3$  out of  $\text{C}_3\text{O}_5\text{O}_4$  plane. See Figure 1 for atom numbering.

<sup>h</sup>A positive displacement occurs when the  $\text{C}_1$  atom moves towards the viewer who sees the atoms 1,4,5 in a counter-clockwise order.

uncertainties of the two sets of data, and the small differences are due to slightly different LSR procedures. In particular, we performed the LSR directly on the residuals of the moments of inertia, whereas the fit in ref. 5 was to the differences between the rotational constants of each isotopologue and those of the parent. It must be emphasized that the rms residual for  $r_0$ (Fit A) is substantial, 0.724 MHz, and the uncertainties are as large as 0.03 Å [ $r(\text{C}-\text{N})$ ] and 33° [ $\gamma(\text{NH}_2 \text{ wag})$ ]. When isotopologues for the [OH,NDH] and [OD,NDH] substitutions are excluded, as in  $r_0$ (Fit B) of Table 7, the rms residual decreases to 0.438 MHz. A significant decrease also occurs in the uncertainties of the individual structural parameters, with standard errors in  $r_0$ (Fit B) less than half of those of  $r_0$ (Fit A). These observations contributed to the decision to exclude the [OH,NDH] and [OD,NDH] isotopologues in all subsequent least-squares refinements.

For our  $r_c$  fits, we used the all-electron 6-31G\* MP2 vibrational corrections with the Gly-**II** empirical rotational constants.

The total zero-point vibrational (ZPV) corrections for Gly-**I**p, Gly-**II**p, and Gly-**II**n are listed in Tables 8 and 9. It is important to note the significant difference in ZPV corrections for Gly-**II**p and Gly-**II**n. Because the experimental rotational constants correspond to a vibrationally averaged planar structure,<sup>3,5</sup> we attempted to perform a LSR on planar Gly-**II**. The Gly-**II**p cc-pVTZ CCSD(T) equilibrium structure and Gly-**II**p 6-31G\* MP2 vibrational corrections were employed in conjunction with the set of empirical rotational constants available for Gly-**II**. The rms residual (0.598 MHz) for this unconstrained fit of the planar Gly-**II**p structure was 37% larger than in  $r_0$ (Fit B) and could not be reduced further. If instead the zero-point vibrational corrections from the nonplanar Gly-**II**n cubic force field are used with experimental rotational constants in a planar fit, the rms residual is even larger, 2.25 MHz. We conclude that a satisfactory fit cannot be obtained unless the structure of Gly-**II** is allowed to be nonplanar and Gly-**II**n vibrational corrections are adopted.



**Table 8.** Zero-Point Vibrational Corrections (in MHz) to Rotational Constants of Gly-**I<sub>p</sub>** Isotopologues Obtained at the All-Electron 6-31G\* MP2 Level.

	$A_e-A_0$	$B_e-B_0$	$C_e-C_0$
Parent	78.67	31.30	22.33
$^{13}\text{C}(3)$	77.80	30.95	22.06
$^{13}\text{C}(1)$	76.73	30.95	21.92
$\text{C}(1)\text{-d}_2$	69.84	31.21	21.48
$^{15}\text{N}$	78.76	30.13	21.71

Gly-**IIn** has  $C_1$  point-group symmetry and thus considerably more structural parameters than Gly-**I<sub>p</sub>**, 24 vs. 15. To determine candidates for constraint release, the same procedure based on determinants of the least-squares Hessian was used as for Gly-**I<sub>p</sub>**. Releasing variables one by one, we obtained the preliminary fit designated as  $r_e(\text{Fit 1})$  in Table 7. The standard errors for the parameters in  $r_e(\text{Fit 1})$  are reduced compared to those in  $r_0(\text{Fit A})$  and  $r_0(\text{Fit B})$ , and the rms residual decreased to 0.303 MHz. Remarkably, the variables for  $r_e(\text{Fit 1})$  differ from the all-electron cc-pVTZ CCSD(T) structural parameters by at most 0.004 Å for bond lengths and 1.7° for angles, with the exception of  $r(\text{O-H})$ , where the difference is 0.019 Å.

The statistical uncertainties and rms deviations can be further reduced by releasing two more parameters,  $\gamma(\text{NH}_2 \text{ wag})$  and  $\Delta\theta(\text{NH}_2 \text{ rock})$ , giving  $r_e(\text{Fit 2})$  in Table 7. The uncertainties of  $r_e(\text{Fit 2})$  are less than 0.002 Å for bond lengths and 1° for valence bond angles. The uncertainties are larger for the torsional

and out-of-plane angles, but still less than 1.5°. This represents a huge improvement in the uncertainties for the out-of-plane  $\text{NH}_2$  wag, which were 33° and 13° in  $r_0(\text{Fit A})$  and  $r_0(\text{Fit B})$ , respectively. The standard errors of  $r_e(\text{Fit 2})$  are the smallest of all LSR procedures of Gly-**IIn**, and the rms residual (52.9 kHz) is drastically smaller than those for  $r_0(\text{Fit A})$ ,  $r_0(\text{Fit B})$ , and  $r_e(\text{Fit 1})$ .

Finally, we released the angle  $\gamma(\text{COOH wag})$  to obtain  $r_e(\text{Fit 3})$  in Table 7. The rms residual of  $r_e(\text{Fit 3})$  diminished to 51.6 kHz, but the uncertainties increased slightly for Fit 3 as compared to Fit 2. Inspecting determinants of the least-squares Hessian shows that no other parameters are determined well enough by the experimental data to be released, and  $r_e(\text{Fit 3})$  is thus our final fit for Gly-**IIn**. The all-electron cc-pVTZ CCSD(T) constraints involved in  $r_e(\text{Fit 3})$  are listed in Table 5. Because the experimental dataset does not contain distinct NHD and CHD monodeuterated isotopologues, the differences  $\Delta r(\text{N-H}) = r(\text{N}_2\text{-H}_{10}) - r(\text{N}_2\text{-H}_9)$  and  $\Delta r(\text{C-H}) = r(\text{C}_1\text{-H}_8) - r(\text{C}_1\text{-H}_7)$  are not well determined from the experimental data and therefore have been constrained.

As seen in Table 7, deviations between the empirically based equilibrium bond lengths of  $r_e(\text{Fit 3})$  and the all-electron cc-pVTZ CCSD(T) distances are smaller than (or equal to) 0.005 Å, except for  $r(\text{O-H})$ , where the deviation is 0.015 Å. For the angles, the situation is somewhat more complicated. It is comforting that the deviations between  $r_e(\text{Fit 3})$  and cc-pVTZ CCSD(T) for the valence bending angles  $\theta(\text{C-O-H})$ ,  $\theta(\text{C-C-O})$ ,  $\theta(\text{O-C-O})$ ,  $\theta(\text{C-C-N})$ ,  $\theta(\text{CH}_2 \text{ scissor})$ , and  $\theta(\text{NH}_2 \text{ scissor})$  are all smaller than 0.8°. For  $\Delta\theta(\text{CH}_2 \text{ wag})$  and  $\Delta\theta(\text{NH}_2 \text{ rock})$  the disparities are 2.4° and 7.6°, respectively. This is not surprising since the fit did not include monodeuter-

**Table 9.** Zero-Point Vibrational Corrections (in MHz) to Rotational Constants of Gly-**I<sub>p</sub>** and Gly-**IIn** Isotopologues Obtained at the All-Electron 6-31G\* MP2 Level.

	Gly- <b>I<sub>p</sub></b> <sup>a</sup>			Gly- <b>IIn</b>		
	$A_e-A_0$	$B_e-B_0$	$C_e-C_0$	$A_e-A_0$	$B_e-B_0$	$C_e-C_0$
Parent	95.88	22.47	21.11	65.73	33.87	32.36
$^{15}\text{N}$	95.75	21.81	20.56	64.97	32.96	31.61
$^{13}\text{C}(3)$	93.99	22.25	20.85	65.01	33.20	31.95
$^{13}\text{C}(1)$	95.02	22.14	20.84	64.85	33.58	32.08
$\text{C}=\text{O}^{18}$	95.45	20.85	19.98	63.60	32.05	30.81
$\text{H}-\text{O}^{18}$	87.02	22.54	20.67	60.90	33.64	31.45
OD, $\text{NH}_2$	92.21	22.87	21.07	60.07	33.68	31.38
$\text{CD}_2$	84.62	22.17	20.36	64.79	31.35	30.45
OH, $\text{NH}(10)\text{D}(9)$	93.97	20.29	19.43	51.14	35.92	34.15
OH, $\text{NH}(9)\text{D}(10)$	93.97	20.29	19.43	78.05	28.39	26.96
OH, $\text{ND}_2$	89.41	19.44	18.90	63.77	30.70	29.00
OD, $\text{NH}(10)\text{D}(9)$	89.81	20.67	19.36	46.80	35.51	33.05
OD, $\text{NH}(9)\text{D}(10)$	89.81	20.67	19.36	70.77	28.35	26.23
OD, $\text{ND}_2$	85.18	19.80	18.82	57.90	30.44	28.14

<sup>a</sup>In order to mimic a zero-point averaged planar structure, VPT2 was applied to the Gly-**I<sub>p</sub>** cubic force field with a mass-weighted Cartesian quadratic force constant matrix modified to be positive definite by performing a spectral decomposition in terms of the normal-mode eigenvectors and changing the sign of the  $\nu_{24}(d'')$  eigenvalue from negative to positive.

ated CHD and NHD isotopologues. A substantial difference of  $4.0^\circ$  is also found for  $\gamma(\text{NH}_2 \text{ wag})$ , which measures the extent of pyramidalization of the amine group. Despite these issues, the central measures of nonplanarity of Gly-**II**n,  $\tau(\text{NCCO}) = (11.2 \pm 1.9)^\circ$ , and  $\tau(\text{CCOH}) = (-2.5 \pm 1.9)^\circ$  are in striking agreement with the corresponding cc-pVTZ CCSD(T) angles of  $12.8^\circ$  and  $-2.3^\circ$ , respectively. Even the empirical estimate of  $\gamma(\text{COOH wag}) = (0.12 \pm 2.86)^\circ$  is consistent with the CCSD(T) value of  $-1.3^\circ$ . In summary, our analysis clearly shows that the experimentally observed rotational constants of Gly-**II** do support an  $r_e^{\text{BO}}$  structure of  $C_1$  point-group symmetry.

## Conclusions

Through the joint use of accurate computational and spectroscopic structural information, this study provides the most rigorous equilibrium structures to date of the two lowest-energy conformers of free glycine. It has been established that while the lowest-energy conformer of neutral glycine, Gly-**I**p, has a planar equilibrium structure, the second lowest-energy conformer, Gly-**II**n, has a nonplanar  $r_e$  structure. A definitive Gly-**II**n barrier to planarity of  $20.5 \pm 5.0 \text{ cm}^{-1}$  has been obtained through high-level ab initio computations with focal-point extrapolations. While the ground vibrational state of Gly-**II**n surely surmounts this classical barrier, we find clear evidence of an underlying nonplanar equilibrium structure in the observed rotational constants. Remarkably, the central measures of nonplanarity of Gly-**II**n,  $\tau(\text{NCCO}) = (-11.2 \pm 1.9)^\circ$  and  $\tau(\text{CCOH}) = (-2.5 \pm 1.9)^\circ$ , are in accord with the cc-pVTZ CCSD(T) predictions to within the standard error of the  $r_e$  fit. The high-precision equilibrium structure of glycine determined here and that of proline determined in ref. 15 show clear differences in bonding in these amino acids, e.g.,  $r_e(\text{C}-\text{N})$  in Pro-**I** is longer by  $0.032 \text{ \AA}$  than in Gly-**I**p.

The use of high-resolution experimental rotational constants and theoretical vibration-rotation interaction constants to determine accurate  $r_e$  structures has a history of notable successes from several pioneering investigators.<sup>15,16,19,20,30,43a,51-60</sup> An excellent demonstration of the power of this approach is the work in 2001 of Bak et al.<sup>16</sup> on 19 small, closed-shell molecules containing first-row atoms. Our ongoing investigations on the equilibrium structures of amino acids in the gas phase, now including both the glycine and proline<sup>15</sup> prototypes, are pushing this methodology into the realm of much more complex and flexible molecules. The Gly-**I**p isomer is an unqualified success in this endeavor. Even in the problematic Gly-**II** case, the key measures of nonplanarity appear to be extracted successfully by the VPT2  $\alpha_i$  approach. However, new experimental analyses of the microwave spectra of the asymmetric NHD isotopologues of Gly-**II**n and more sophisticated theoretical treatments to better account for large-amplitude motions of this species in a double-well potential should prove instructive.

## Acknowledgments

Computations were performed in part using the Molecular Science Computing Facility (MSCF) in the William R. Wiley Environmental Molecular Sciences Laboratory, a national scientific

user facility sponsored by the U.S. Department of Energy's Office of Biological and Environmental Research and located at the Pacific Northwest National Laboratory, operated for the Department of Energy by Battelle. We thank Nicholas Marshall for his help in resolving several computational issues.

## References

1. Combes, F.; Nguyen-Q-Rien; Wlodarczak, G. *Astron Astrophys* 1996, 308, 618.
2. Brown, R. D.; Godfrey, P. D.; Storey, J. W. V.; Bassez, M. P. *J Chem Soc Chem Commun* 1978, 547.
3. Godfrey, P. D.; Brown, R. D. *J Am Chem Soc* 1995, 117, 2019.
4. Iijima, K.; Tanaka, K.; Onuma, S. *J Mol Struct* 1991, 246, 257.
5. McGlone, S. J.; Elmes, P. S.; Brown, R. D.; Godfrey, P. D. *J Mol Struct* 1999, 486, 225.
6. Suenram, R. D.; Lovas, F. J. *J Mol Spectrosc* 1978, 72, 372.
7. Császár, A. G. *J Am Chem Soc* 1992, 114, 9568.
8. Császár, A. G. *J Mol Struct* 1995, 346, 141.
9. Császár, A. G.; Perczel, A. *Prog Biophys Mol Biol* 1999, 71, 243.
10. Hu, C.-H.; Shen, M.; Schaefer, H. F. *J Am Chem Soc* 1993, 115, 2923.
11. Sellers, H. L.; Schäfer, L. *J Am Chem Soc* 1978, 100, 7728.
12. Stepanian, S. G.; Reva, I. D.; Radchenko, E. D.; Rosado, M. T. S.; Duarte, M. L. T. S.; Fausto, R.; Adamowicz, L. *J Phys Chem A* 1998, 102, 1041.
13. Vishveshwara, S.; Pople, J. A. *J Am Chem Soc* 1977, 99, 2422.
14. Schäfer, L.; Sellers, H. L.; Lovas, F. J.; Suenram, R. D. *J Am Chem Soc* 1980, 102, 6566.
15. Allen, W. D.; Czinki, E.; Császár, A. G. *Chem Eur J* 2004, 10, 4512.
16. Bak, K. L.; Gauss, J.; Jørgensen, P.; Olsen, J.; Helgaker, T.; Stanton, J. F. *J Chem Phys* 2001, 114, 6548.
17. Halkier, A.; Jørgensen, P.; Gauss, J.; Helgaker, T. *Chem Phys Lett* 1997, 274, 235.
18. Helgaker, T.; Gauss, J.; Jørgensen, P.; Olsen, J. *J Chem Phys* 1997, 106, 6430.
19. Allen, W. D.; Yamaguchi, Y.; Császár, A. G.; Clabo, D. A., Jr.; Remington, R. B.; Schaefer, H. F. *Chem Phys* 1990, 145, 427.
20. Clabo, D. A., Jr.; Allen, W. D.; Remington, R. B.; Yamaguchi, Y.; Schaefer, H. F. *Chem Phys* 1988, 123, 187.
21. Nielsen, H. H. *Rev Mod Phys* 1951, 23, 90.
22. Papoušek, D.; Aliev, M. R. *Molecular Vibrational-Rotational Spectra*; Elsevier: Amsterdam, 1982.
23. Watson, J. K. G. In *Vibrational Spectra and Structure*, Vol. 6; Durig, J. R., Ed.; Elsevier: Amsterdam, 1997; p. 1.
24. Dunning, T. H., Jr. *J Chem Phys* 1989, 90, 1007.
25. Hampel, C.; Peterson, K.; Werner, H.-J. *Chem Phys Lett* 1992, 190, 1.
26. Purvis, G. D., III; Bartlett, R. J. *J Chem Phys* 1982, 76, 1910.
27. Raghavachari, K.; Trucks, G. W.; Pople, J. A.; Head-Gordon, M. *Chem Phys Lett* 1989, 157, 479.
28. Werner, H.-J.; Knowles, P. J.; Schütz, M.; Lindh, R.; Celani, P.; Korona, T.; Rauhut, G.; Manby, F. R.; Amos, R. D.; Bernhardsson, A.; Berning, A.; Cooper, D. L.; Deegan, M. J. O.; Dobbyn, A. J.; Eckert, F.; Hampel, C.; Hetzer, G.; Lloyd, A. W.; McNicholas, S. J.; Meyer, W.; Mura, M. E.; Nicklaß, A.; Palmieri, P.; Pitzer, R. M.; Schumann, U.; Stoll, H.; Stone, A. J.; Tarroni, R.; Thorsteinsson, T. *MOLPRO*, version 2002.1, Birmingham, U.K.
29. Stanton, J. F.; Gauss, J.; Watts, J. D.; Szalay, P. G.; Bartlett, R. J., Mainz-Austin-Budapest (MAB) version of ACESII, with contributions from Auer, A. A.; Bernholdt, D. B.; Christiansen, O.; Harding, M. E.; Heckert, M.; Heun, O.; Huber, C.; Jonsson, D.; Jusélius, J.; Lauderdale, W. J.; Metzroth, T.; Michauk, C.; Ruud, K.; Schiffmann, F.; Tajti, A. and the integral packages: MOLECULE (Almlöf, J. and

- Taylor, P. R.), PROPS (Taylor, P. R.), and ABACUS (Helgaker, T.; Aa. Jensen, H. J.; Jørgensen, P.; Olsen, J.). See also Stanton, J. F.; Gauss, J.; Watts, J. D.; Lauderdale, W. J.; Bartlett, R. J. *Int J Quantum Chem Symp* 1992, 26, 879. The current version is available at [www.aces2.de](http://www.aces2.de).
30. Allen, W. D.; East, A. L. L.; Császár, A. G. In *Structures and Conformations of Non-Rigid Molecules*; Laane, J.; Dakkouri, M.; van der Veken, B.; Oberhammer, H., Eds.; Kluwer: Dordrecht, 1993; p. 343.
  31. Császár, A. G.; Allen, W. D.; Schaefer, H. F. *J Chem Phys* 1998, 108, 9751.
  32. Császár, A. G.; Tarczay, G.; Leininger, M. L.; Polyansky, O. L.; Tennyson, J.; Allen, W. D. In *Spectroscopy from Space*, Demaison, J.; Sarka, K. Eds.; Kluwer: Dordrecht, 2001; p. 317.
  33. East, A. L. L.; Allen, W. D. *J Chem Phys* 1993, 99, 4638.
  34. Gonzales, J. M.; Pak, C.; Cox, R. S.; Allen, W. D.; Schaefer, H. F.; Tarczay, G.; Császár, A. G. *Chem Eur J* 2003, 9, 2173.
  35. Feller, D. *J Chem Phys* 1992, 96, 6104.
  36. Feller, D. *J Chem Phys* 1993, 98, 7059.
  37. Helgaker, T.; Klopper, W.; Koch, H.; Noga, J. *J Chem Phys* 1997, 106, 9639.
  38. Kendall, R. A.; Dunning, T. H., Jr.; Harrison, R. J. *J Chem Phys* 1992, 96, 6796.
  39. Wilson, A. K.; van Mourik, T.; Dunning, T. H., Jr. *J Mol Struct* 1996, 388, 339.
  40. (a) Woon, D. E.; Dunning, T. H., Jr. *J Chem Phys* 1993, 98, 1358; (b) Woon, D. E.; Dunning, T. H., Jr. *J Chem Phys* 1994, 100, 2975.
  41. Woon, D. E.; Dunning, T. H., Jr. *J Chem Phys* 1995, 103, 4572.
  42. Schneider, W.; Thiel, W. *Chem Phys Lett* 1989, 157, 367.
  43. (a) Stanton, J. F.; Gauss, J. *Int Rev Phys Chem* 2000, 19, 61; (b) Stanton, J. F.; Lopreore, C.; Gauss, J. *J Chem Phys* 1998, 108, 7190.
  44. Hariharan, P. C.; Pople, J. A. *Theor Chim Acta* 1973, 28, 213.
  45. Handy, N. C.; Amos, R. D.; Gaw, J. F.; Rice, J. E.; Simandiras, E. D. *Chem Phys Lett* 1985, 120, 151.
  46. Allen, W. D.; Császár, A. G. *J Chem Phys* 1993, 98, 2983.
  47. DeKock, R. L.; McGuire, M. J.; Piecuch, P.; Allen, W. D.; Schaefer, H. F.; Kowalski, K.; Kucharski, S. A.; Musial, M.; Bonner, A. R.; Spronk, S. A.; Lawson, D. B.; Laursen, S. L. *J Phys Chem A* 2004, 108, 2893.
  48. Allen, W. D.; Császár, A. G. *J Chem Phys* 1993, 98, 2983.
  49. Allen, W. D.; Császár, A. G.; Szalay, V.; Mills, I. M. *Mol Phys* 1996, 89, 1213.
  50. Sarka, K.; Demaison, J. In *Computational Molecular Spectroscopy*; Jensen, P.; Bunker, P. R., Eds.; Wiley: Chichester, 2000; pp. 255–303.
  51. East, A. L. L.; Allen, W. D.; Klippenstein, S. J. *J Chem Phys* 1995, 102, 8506.
  52. East, A. L. L.; Johnson, C. S.; Allen, W. D. *J Chem Phys* 1993, 98, 1299.
  53. Thiel, W.; Scuseria, G.; Schaefer, H. F.; Allen, W. D. *J Chem Phys* 1988, 89, 4965.
  54. Pulay, P.; Meyer, W.; Boggs, J. E. *J Chem Phys* 1978, 68, 5077.
  55. Gauss, J.; Stanton, J. F. *J Phys Chem A* 2000, 104, 2865.
  56. McCarthy, M. C.; Gottlieb, C. A.; Thaddeus, P.; Horn, M.; Botschwina, P. *J Chem Phys* 1995, 103, 7820.
  57. Bartel, C.; Botschwina, P.; Bürger, H.; Guarnieri, A.; Heyl, A.; Huckauf, A.; Lentz, D.; Merzliak, T.; Mkdami, E. B. *Angew Chem Int Ed* 1998, 37, 2879.
  58. Pawlowski, F.; Jørgensen, P.; Olsen, J.; Hegelund, F.; Helgaker, T.; Gauss, J.; Bak, K. L.; Stanton, J. F. *J Chem Phys* 2002, 116, 6482.
  59. Carter, S.; Mills, I. M.; Handy, N. C. *J Chem Phys* 1992, 97, 1606.
  60. Demaison, J.; Włodarczak, G.; Rudolph, H. D. *Adv Mol Struct Res* 1997, 3, 1.